

## *J/ψ* suppression in central Pb–Pb collisions

P. M. Dinh<sup>a</sup>[SPhT]Service de physique théorique, CEA-Saclay, F-91191 Gif-sur-Yvette cedex, J.-P. Blaizot<sup>b</sup>[SPhT]\*, and J.-Y. Ollitrault<sup>c</sup>[SPhT]\*

<sup>a</sup>[

We discuss the recent NA50  $J/\psi$  production data in Pb–Pb collisions, in particular the second drop at high transverse energies which correspond to the most central collisions. Using a model which relates the  $J/\psi$  suppression to the local energy density, we show that the data can be explained by taking into account transverse energy fluctuations at a given impact parameter. Predictions of this model for RHIC are briefly discussed.

### 1. Introduction

The rate of  $J/\psi$  production in  $p$ - $p$ ,  $p$ - $A$  and  $A$ - $B$  collisions involving oxygen and sulphur projectiles is well understood in terms of a hard production of the  $c\bar{c}$  pair followed by nuclear absorption [1,2]. In Pb–Pb collisions, however, evidence for an additional suppression mechanism, the so-called anomalous suppression, has been obtained by the NA50 collaboration [3]. Furthermore, in the recent NA50 data [4] a second drop in the pattern of the  $J/\psi$  production occurs at high transverse energy ( $E_T$ ), that is, for the most central collisions. The origin of this second drop is the focus of this contribution.

### 2. Improved geometrical model

It is possible to explain the anomalous  $J/\psi$  suppression by using a scenario [5] which relates it to the local energy density  $\epsilon$ . More precisely, we formulate a simple geometrical model in which final state interactions suppress all the  $J/\psi$ 's originating from  $c\bar{c}$  pairs produced in a region where the local energy density  $\epsilon$  exceeds some critical threshold  $\epsilon_c$ . We then assume that the local energy density is proportional to the density  $n_p$  of participant nucleons per unit area (transverse to the collision axis) calculated in a Glauber model [6]: the total transverse energy is then proportional to the number of participants, as observed experimentally. In such a model, the suppression criterion depends only on the impact parameter (through  $n_p$ ), so that the  $J/\psi$  suppression saturates at high  $E_T$  where the impact parameter is essentially zero (see the short-dashed curve in Fig.1b). A clear deviation from this simple behavior is seen in the most recent NA50 data.

A better description is obtained by taking into account the fluctuations of  $E_T$  for a given impact parameter  $b$  [2]. These fluctuations are an essential component of the tail of the  $E_T$  distribution (see Fig.1a). As a simple ansatz, we take the distribution of  $E_T$  at fixed  $b$  to be a gaussian with mean value  $\langle E_T \rangle(\mathbf{b}) = qN_p(\mathbf{b})$ , where  $N_p(b) = \int d^2\mathbf{s} n_p(\mathbf{s}, \mathbf{b})$

---

\*Member of CNRS

is the total number of participants at impact parameter  $\mathbf{b}$  and  $n_p(\mathbf{s}, \mathbf{b})$  the corresponding density per unit area at the transverse coordinate  $\mathbf{s}$ . The dispersion of the gaussian is given by  $\sigma_{E_T}^2 = aq^2 N_p(\mathbf{b})$ , with  $a$  a dimensionless parameter. The values of the fit parameters  $q = 0.274$  GeV and  $a = 1.27$  are those determined by the NA50 collaboration [7].

Part of the  $E_T$  fluctuations is physical, part is due to the intrinsic resolution of the NA50 electromagnetic calorimeter. The latter is given by  $\sigma_{\text{intrinsic}}(E_T)/E_T = \alpha/\sqrt{E_T} + \beta$ , with  $\alpha \simeq 0.2$  GeV $^{1/2}$  and  $\beta \simeq 0.005$  [8]. The physical  $E_T$  fluctuations  $\sigma_{\text{phys}} = \sqrt{\sigma_{E_T}^2 - \sigma_{\text{intrinsic}}^2}$  [7] thus differ only by 10% from the observed fluctuations  $\sigma_{E_T}$  for central collisions ( $E_T \sim 100$  GeV), so that we neglect the intrinsic resolution in what follows.

In order to take into account the  $E_T$  fluctuations, we replace the previous estimate  $\epsilon \propto n(\mathbf{s}, \mathbf{b})$  [5], with the more accurate  $\epsilon \propto (E_T/\langle E_T \rangle(\mathbf{b}))n_p(\mathbf{s}, \mathbf{b})$  [9]. Thus for a given impact parameter, the energy density is proportional to  $E_T$  [10]. With this prescription, the average energy density in the collision area  $S$ , defined by  $\langle \epsilon \rangle \equiv (1/S) \int_S \epsilon(\mathbf{s}, \mathbf{b}) d^2\mathbf{s}$ , is proportional to  $E_T/S$ , in agreement with the traditional Bjorken estimate [11].

### 3. Comparison with NA50 data

It is easy to understand that this improvement leads to an increased suppression at high  $E_T$ . Indeed, at high  $E_T$  where the geometry of the collision is essentially fixed at zero impact parameter, the local energy density  $\epsilon$  scales like  $E_T$  and the region where it exceeds  $\epsilon_c$  becomes bigger and bigger as  $E_T$  increases.

This model reproduces the main features of the  $J/\psi$  production pattern observed by NA50; however, it does not provide a perfect fit to the data [9]. A better description is obtained if we allow for two thresholds, in line with the idea of successive meltings of the  $\chi$  and the  $J/\psi$  (full curve in Fig.1b). However we should emphasize that an identically good fit is obtained for a grad-

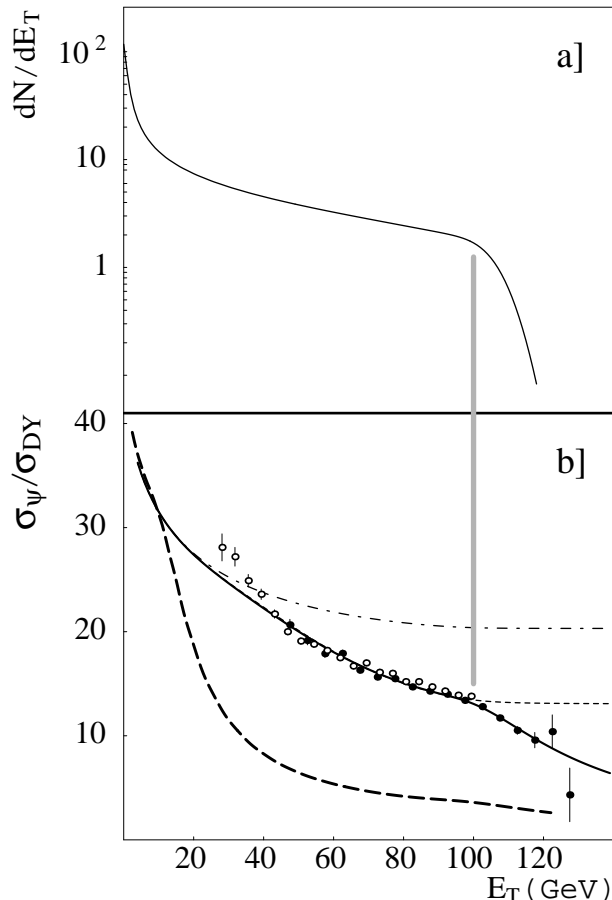


Figure 1: a) Minimum bias  $E_T$ -distribution. b)  $J/\psi$  over Drell-Yan production ratio as a function of  $E_T$ . Open (resp. closed) circles: NA50 1996 (resp. 1998) data. Dotted-dashed curve: nuclear absorption alone. Full curve (resp. short dashes): our model for anomalous suppression with (resp. without)  $E_T$  fluctuations. Long dashes: prediction for Au–Au collisions at RHIC energies (see text). The vertical line sets the position of the knee of the  $E_T$ -distribution, where the second drop occurs in the ratio.

ual suppression above a single threshold. Therefore the structure in the pattern of  $J/\psi$  suppression cannot be interpreted as a signal of the successive meltings of charmonium resonances. In any case, we stress that the convolution of the suppression factor with the impact parameter distribution (for a given  $E_T$ ) and the energy density profile in the interaction region tends to smoothen any threshold, even that associated with the onset of the anomalous suppression at lower  $E_T$ .

Whatever the chosen scenario and/or the value of the thresholds, we always obtain a second drop starting around the knee of the  $E_T$ -distribution, which directly reflects the effect of  $E_T$  fluctuations. Note that in order to account for the data, all the  $J/\psi$ 's must be suppressed at the highest energy densities.

We have estimated the average transverse momentum squared of the produced  $J/\psi$ 's as a function of  $E_T$ . Analogous computations have been done in [12] and we reproduce the behavior predicted there: at low  $E_T$ ,  $\langle p_T^2 \rangle$  increases rapidly due to initial state scattering of the  $c\bar{c}$  pair [13]; this increase saturates when anomalous suppression sets in, and  $\langle p_T^2 \rangle$  eventually decreases above the knee of the  $E_T$  distribution. Compared to the calculation in [12], this decrease is amplified by  $E_T$  fluctuations. This behavior is not compatible with the centrality dependence of  $\langle p_T^2 \rangle$  recently measured by NA50 [14]. Indeed the data show a monotonous increase with  $E_T$ . Note however that our suppression criterion is  $p_T$ -independent, while various arguments lead us to expect that a  $J/\psi$  with a high  $p_T$  is to be less suppressed. The implementation of such effects is under way [15].

#### 4. Predictions for RHIC

The recent PHOBOS measurement [16] shows that the total multiplicity is larger by 70% at RHIC than at SPS in central collisions. We thus assume that the energy density is also increased by 70% at RHIC. The above model then yields a parameter free prediction for Au-Au collisions at RHIC, which is plotted as the long-dashed curve in Fig.1b. In order to compare RHIC and SPS results, we have rescaled the RHIC tranverse energy so that the knees of the two distributions coincide. In the Glauber model formulas, we use the value of the nucleon-nucleon inelastic cross section  $\sigma_{NN} = 41$  mb at RHIC energies, instead of  $\sigma_{NN} = 32$  mb at SPS energies.

We have assumed so far that the energy density scales with the density of participants, i.e.  $\epsilon \propto n_p(\mathbf{b}, \mathbf{s})E_T/\langle E_T \rangle(\mathbf{b})$ ; this was a consequence of the observation that multiplicities and transverse energies approximately scale with the number of participants at SPS. But at RHIC energies, a so-called “hard” component appears which gives rise to an additional term, proportional to number of binary collisions [10,17]. The density per unit transverse area of binary collisions is  $n_{bin}(\mathbf{b}, \mathbf{s}) \propto T_A(\mathbf{s})T_B(\mathbf{b} - \mathbf{s})$ , where  $T_A(\mathbf{s})$  is the nucleus profile function, and this term must be taken into account in evaluating the energy density. We have checked numerically that this does not change qualitatively our predictions for  $J/\psi$  suppression.

Since the energy density is significantly larger at RHIC than at SPS, the anomalous suppression sets in earlier. Around the knee, the suppression for Au–Au collisions is about 2.5 times greater than at SPS for Pb–Pb collisions, so that the effect of  $E_T$  fluctuations, although still visible, is much reduced. In a smaller system, e.g. Ca–Ca, the  $J/\psi$  suppression would be roughly the same at RHIC as the Pb–Pb system at SPS. Note, however,

that the present model ignores the possibility that several  $c\bar{c}$  pairs may be produced in the collision. As recently shown [18], this may lead to an enhancement of  $J/\psi$  production at RHIC, and may mask the suppression mechanism discussed here.

### Acknowledgments

We thank Bernard Chaurand for detailed explanations concerning the NA50 analysis.

### REFERENCES

1. A. Capella *et al.*, Phys. Lett. **B206** (1988) 354; C. Gerschel and J. Hüfner, Z. Phys. **C56** (1992) 171.
2. D. Kharzeev, C. Lourenco, M. Nardi and H. Satz, Z. Phys. C **74** (1997) 307.
3. M. Gonin *et al.* [NA50 Collaboration], Nucl. Phys. **A610**, 404c (1996).
4. M. C. Abreu *et al.* [NA50 Collaboration], Phys. Lett. **B477** (2000) 28.
5. J. P. Blaizot and J. Y. Ollitrault, Phys. Rev. Lett. **77**, 1703 (1996).
6. R. J. Glauber and G. Matthiae, Nucl. Phys. **B21** (1970) 135; A. Bialas *et al.*, Nucl. Phys **B111** (1976) 104.
7. B. Chaurand, private communication.
8. I. Chevrot, “Etude du flot en fonction de la centralité dans les collisions d’ions lourds aux énergies ultrarelativistes”, Doctorat de l’université Blaise Pascal, Clermont-Ferrand, 1998.
9. J. P. Blaizot, P. M. Dinh and J. Y. Ollitrault, Phys. Rev. Lett. **85**, 4012 (2000).
10. A. Capella, E. G. Ferreiro and A. B. Kaidalov, Phys. Rev. Lett. **85**, 2080 (2000).
11. J. D. Bjorken, Phys. Rev. D **27** (1983) 140.
12. D. Kharzeev, M. Nardi and H. Satz, Phys. Lett. B **405** (1997) 14.
13. S. Gavin and M. Gyulassy, Phys. Lett. B **214** (1988) 241; J. Hufner, Y. Kurihara and H. J. Pirner, Phys. Lett. B **215** (1988) 218; J. P. Blaizot and J. Y. Ollitrault, Phys. Lett. B **217** (1989) 392.
14. M. C. Abreu *et al.* [NA50 Collaboration], CERN-EP-2000-141.
15. J.-P. Blaizot, P.M. Dinh and J.-Y. Ollitrault, work in progress.
16. B. B. Back *et al.* [PHOBOS Collaboration], Phys. Rev. Lett. **85** (2000) 3100.
17. D. Kharzeev and M. Nardi, nucl-th/0012025.
18. P. Braun-Munzinger and J. Stachel, Phys. Lett. B **490** (2000) 196; R. L. Thews, M. Schroedter and J. Rafelski, hep-ph/0007323.